Research Paper

Theranostic Nucleic Acid Binding Nanoprobe Exerts Anti-inflammatory and Cytoprotective Effects in Ischemic Injury

Howard H. Chen[1, 2], Hushan Yuan[3], Hoonsung Cho[3], Yan Feng[4], Soeun Ngoy[5], Anand T. N. Kumar[1], Ronglih Liao[5], Wei Chao[4], Lee Josephson[1, 3], David E. Sosnovik[1, 2✉]

1. Martinos Center for Biomedical Imaging, Massachusetts General Hospital, Harvard Medical School, Boston MA;
2. Cardiovascular Research Center, Massachusetts General Hospital, Harvard Medical School, Boston MA.
3. Department of Radiology, Massachusetts General Hospital, Harvard Medical School, Boston MA (H.C.: currently School of Materials Science and Engineering, Chonnam National University, Gwangju, South Korea).
4. Department of Anesthesia, Critical Care and Pain Medicine, Massachusetts General Hospital, Harvard Medical School, Boston MA (currently Department of Anesthesiology, University of Maryland School of Medicine, Baltimore MD).
5. Division of Genetics and Division of Cardiovascular Medicine, Department of Medicine, Brigham and Women's Hospital, Harvard Medical School, Boston MA.

✉ Corresponding author: David E. Sosnovik, MD FACC, Martinos Center for Biomedical Imaging, Massachusetts General Hospital and Harvard Medical School, 149 13th St, Boston, MA 02129, VOICE: (617) 724-3407 Email: sosnovik@nmr.mgh.harvard.edu.

Abstract

Extracellular nucleic acids are proinflammatory molecules that have been implicated in a diverse range of diseases. We report here the development of a multivalent nucleic acid scavenging nanoprobe, where the fluorochrome thiazole orange (TO) is conjugated to a polymeric 40 kDa dextran carrier. Dextran-TO (Dex-TO) has nanomolar affinity for mammalian and bacterial nucleic acids and attenuates the production of inflammatory cytokines from activated macrophages exposed to DNA and RNA. Mice with myocardial ischemia reperfusion that were treated with Dex-TO showed a decrease in myocardial macrophage infiltration at 24 hours (p<0.05) and a decrease in infarct size (18% ± 9%, p<0.01) on day 7. Dex-TO allows sites of injury to be identified with fluorescence imaging, while simultaneously exerting an anti-inflammatory and cytoprotective effect. Dex-TO could be of significant diagnostic and therapeutic (theranostic) utility in a broad range of conditions including ischemia, trauma, burns, sepsis and autoimmune disease.

Key words: DNA, RNA, Inflammation, Ischemia, Nanoprobe, Imaging.

Introduction

The release of nucleic acids (NAs) into the extracellular space is a hallmark of cell necrosis and rupture. NA levels are elevated in the serum of patients with sepsis, shock, autoimmune disease, stroke, and acute ischemia, and correlate with the severity of injury [1-6]. The released NAs exacerbate the degree of injury by stimulating an inflammatory response in immune cells [7-9], cardiomyocytes [8, 9], fibroblasts [10] and epithelial cells [11, 12]. This effect is mediated by pattern-recognition receptors, such as Toll-like receptors (TLRs) on immune cells, and plays a central role in innate immunity. We hypothesized

here that the injection of a NA-scavenging nanoprobe would interrupt this process and exert an anti-inflammatory and cytoprotective effect. In addition, we hypothesized that the fluorescent signature of the nanoprobe would allow sites of injury to be identified and the kinetics of NA release to be characterized.

Thiazole-orange (TO) is a vital fluorochrome that binds to NAs but not to serum proteins. We have previously shown that TO can be conjugated to gadolinium chelates and large nanoparticles, such as Feraheme (FH), to create diagnostic imaging agents

[13-15]. These biomaterials, however, have limitations both as diagnostic and therapeutic agents. Gadolinium-TO is monovalent, has a relatively low affinity for NAs and is rapidly cleared by glomerular filtration. On the other hand, the far larger FH-TO nanoparticle exhibits poor tissue penetration and rapid clearance by the cells of the reticulo-endothelial system [16]. In addition, the repeated use of FH-TO is limited by iron's slow excretion and toxicity. Here we describe Dextran-TO (Dex-TO), an iron-free multivalent NA-binding nanoprobe designed to detect, image and scavenge released NAs at sites of injury. While approaches to remove NA such as DNase and polymers relying on electrostatic forces have been described, none possess the specificity and theranostic capability we aimed to achieve here with Dex-TO.

Results

Characterization of Dex-TO

The synthesis of Dex-TO was accomplished by conjugation of a 40 kDa amino-Dextran to the NHS ester of TO (Figure 1A). An average of 3 TOs were present per nanoparticle (Figure 1A). The reaction reached steady state after 3 hours at 37°C, is cost-effective and amendable to scaling up for large-scale synthesis. A parallel reaction was performed between a 40 kDa amino-Dextran and Cy5.5-NHS to yield the Dex-Cy5.5 control nanoparticle (Figure 1B).

Characterization of the probe by flow cytometry showed that Dex-TO was excluded from healthy cells (Fig 1C), but bound to necrotic cells with an affinity similar to commercial vital dyes such as Sytox blue (Figure 1D). Strong nuclear colocalization of Dex-TO and Sytox blue was seen in necrotic cells (Figure 1E). The multivalent nature of Dex-TO markedly enhanced its affinity for NA (Figure 1F). The signal produced by TO, which is indicative of its binding to NA, was significantly higher with Dex-TO than with equivalent concentrations of monovalent TO (TO-PRO). No fluorescence increase was seen when either Dex-Cy5.5 or Cy5.5 was incubated with DNA.

The size of Dex-TO, before and after NA binding, was studied with fast liquid protein chromatography (FPLC) and light scattering. Calibration of Dex-TO (red) against known standards (black) revealed a particle diameter of 4.9 nm (Figure 1G, H). In the presence of NAs, Dex-TO formed complexes up to 250 nm in diameter by light scattering (Figure 1I), which is highly concordant with the cluster size produced by DNA and FH-TO by atomic force microscopy [13].
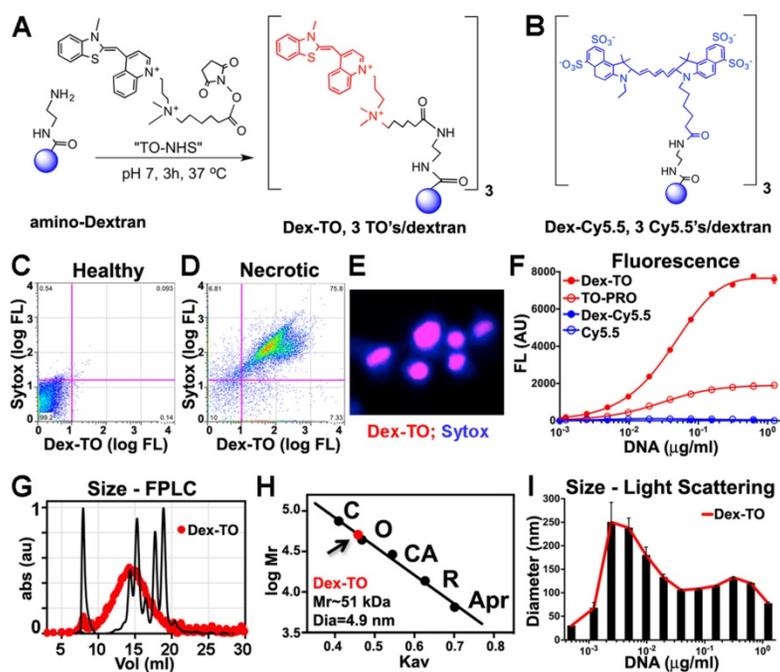

Figure 1: Synthesis and characterization of the Dextran-TO nanoprobe. A. A 40 kDa amino dextran is reacted with the TO-NHS (N-hydroxysuccinimide, shown in red), to yield the Dex-TO nanoprobe with an average of 3 TO per particle. **B.** The control material, Dex-Cy5.5, had an average of 3 Cy5.5 (blue) per particle. **C-D.** Flow cytometry scattergrams of Dex-TO and the reference intravital fluorochrome Sytox-blue show that the Dex-TO nanoprobe is excluded from healthy cells (C), and taken up by sytox positive, necrotic cells (D). **E.** By confocal microscopy Dex-TO uptake is nuclear and colocalizes with sytox. **F.** Dex-TO fluorescence increases steeply with DNA concentration, while substantially less increase is seen with TO-PRO 1 and none with Dex-Cy5.5 or Cy5.5. **G-H.** Dex-TO (red) size was determined by FPLC against known standards, and has a molecular weight of 51 kDa and a diameter of 4.9 nm. **I.** In the presence of DNA, Dex-TO forms multimeric clusters, which reach a size of 200-300 nm by light scattering. FPLC standards: conalbumin (C), ovalbumin (O), carbonic anhydrase (CA), RNase A (R), aprotinin (Apr).

Imaging of Dex-TO binding to NAs

The binding of Dex-TO to NAs was further assessed with fluorescence reflectance imaging (FRI). The addition of NA to a solution of Dex-TO markedly prolonged its fluorescence lifetime, indicative of active binding (Figure 2A). Fluorescence lifetime was also increased in the necrotic tissue of an infarcted mouse heart after the intravenous injection of Dex-TO, while no change was seen with the injection of Dex-Cy5.5 (Figure 2B, C).

The detection of necrotic tissue with Dex-TO was systematically evaluated in acutely infarcted mice (n=7) with continuous wave FRI, due to its wide availability and ease of use. A strong correlation between Dex-TO uptake and infarct area by TTC staining was consistently seen (Figure 2D). In contrast, no correlation was seen between infarction and Dex-Cy5.5 distribution. Receiver operating characteristic (ROC) analysis was performed to determine the segmentation threshold producing the optimal combination of sensitivity and specificity for Dex-TO in the heart, with TTC staining serving as the gold standard. The thresholds tested were defined by the percent increase in signal intensity above the uninjured septum and ranged from 5-35% (Figure 2E). ROC analysis revealed an optimal threshold of 27% and an area under the curve (AUC) of 0.88 (Figure 2F).

Further evaluation of Dex-TO as an imaging agent was performed by comparison with monovalent TO constructs, synthesized as shown in Figure 3A. TO was conjugated to the metal binding chelate DTPA (diethylene triamine pentaacetic acid) as previously described [14]. The uptake of two monovalent metal-TO chelates (Gd-TO and ^{111}In-TO) was quantified in acutely infarcted mice (n=6 per group) and compared with Dex-TO (n=7). These agents form a spectrum of TO constructs (Figure 3B) ranging from small molecules (Gd-TO, ^{111}In-TO) and small nanoparticles (Dex-TO), to large nanoparticles (FH-TO). A mouse injected with Gd-TO and imaged with a conventional gradient echo cine 18 hours after injury is shown in Figure 3C. The contrast generated by this sequence is moderate. In comparison, marked contrast was produced in mice imaged with inversion recovery gradient echo within 24 hours of injury (Figure 3D).

FRI of Dex-TO also produced strong contrast (Figure 3E), but unlike inversion recovery gradient echo, the signal in the septum was not nulled. The biodistribution of ^{111}In-TO showed significantly higher uptake in the infarct than the uninjured septum. The target to background ratios of ^{111}In-TO (2.9 ± 1.3 infarct vs 0.6 ± 0.3 septum, $p<0.0001$) and Dex-TO (1.5 ± 0.2 infarct vs 1.0 ± 0.1 septum, $p<0.001$) were both significantly elevated (Figure 3G). Likewise, both Gd-TO (14.2 ± 3.5) and Dex-TO (33.1 ± 16.1 vs 0 for Dex-Cy5.5, $p<0.0001$) generated a high contrast-to-noise ratio (CNR) between the infarct and the septum (Figure 3H). The tissue contrast generated by Dex-TO thus compared very favorably with Gd-TO and ^{111}In-TO.
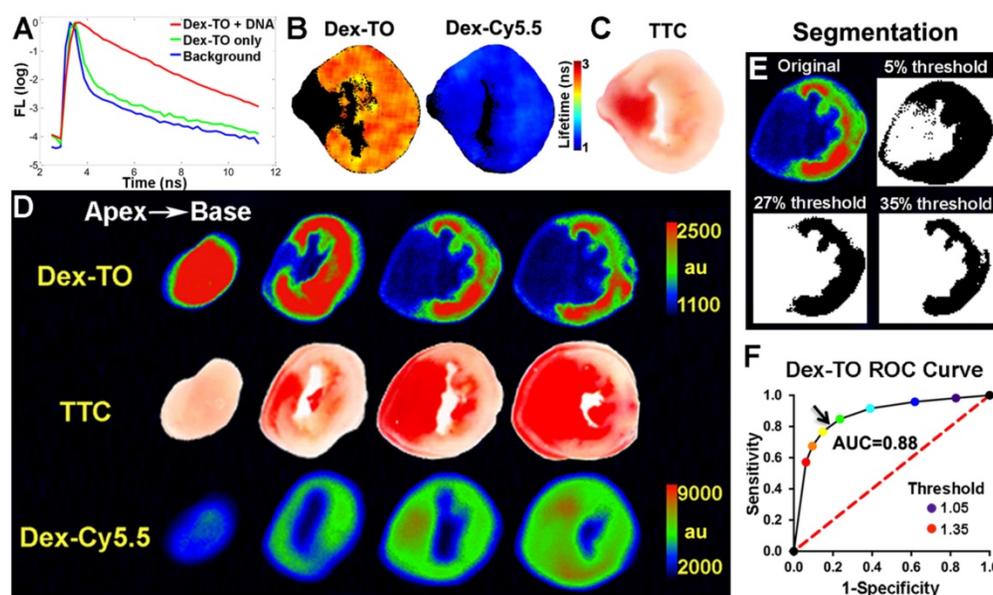

Figure 2: Dex-TO specifically detects extracellular nucleic acid release during acute myocardial infarction. A. Lifetime fluorescence of Dex-TO increases in the presence of DNA. **B.** Lifetime of Dex-TO increases in the anterior wall of the left ventricle (orange to red), but not in the uninjured septum (black). No lifetime change was seen with Dex-Cy5.5. **C.** TTC staining of the same heart slice as in (B). **D.** Continuous wave fluorescence imaging of an infarcted mouse heart after Dex-TO and Dex-Cy5.5 co-injection, followed by TTC staining. Dex-TO uptake is confined to the TTC-negative pale area. No specific uptake was seen with Dex-Cy5.5. **E.** Segmentation of Dex-TO fluorescence by thresholding based on the septal signal from the matching slice. **F.** ROC curve demonstrates that Dex-TO detects necrosis with high sensitivity and specificity (AUC=0.88), with an optimal threshold (arrow) of 27% above the septal signal.
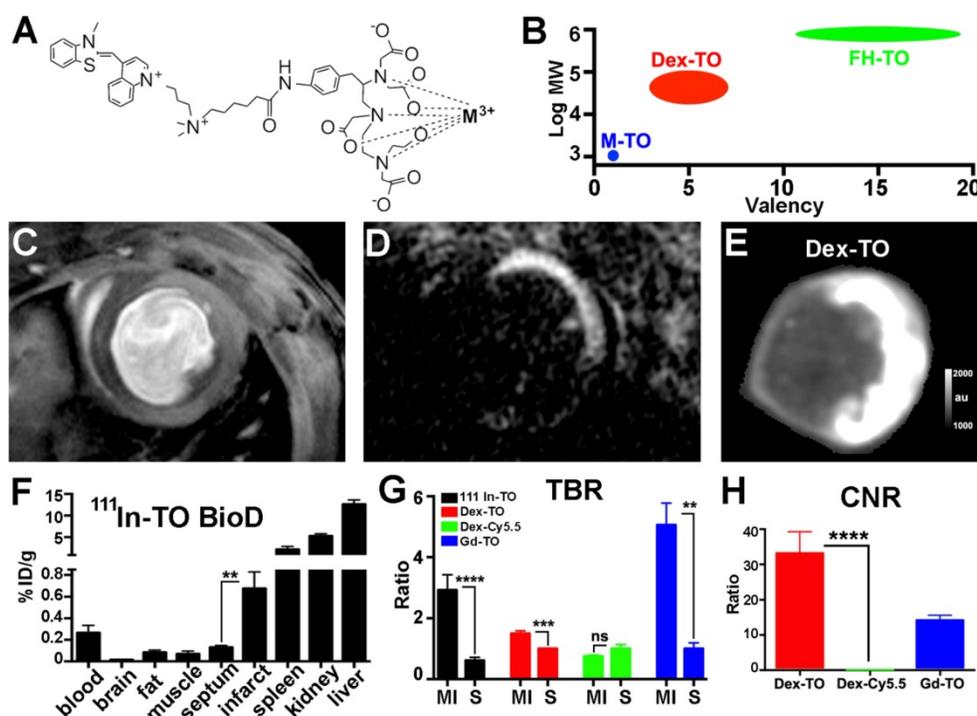
Figure 3: Comparison of small chelates of TO with the Dex-TO nanoprobe. A. Structure of DTPA-TO chelates. Gd-TO is obtained when the metal (M) is Gd^{3+}, and ^{111}In-TO is obtained with $^{111}In^{3+}$ chelation. **B.** M-TOs have a low molecular weight and are monovalent. In contrast, FH-TO forms a very large and highly multivalent nanoparticle. Dex-TO is characterized by intermediate size and multivalency. **C.** Gradient echo cine image of a mouse injected with Gd-TO 18 hours after infarction. Accumulation of the agent in the infarct produces modest contrast. **D.** Inversion recovery gradient echo image of a mouse injected with Gd-TO 14 hours after infarction. Non-infarcted myocardium is nulled producing strong contrast. **E.** Dex-TO fluorescence of a heart 24 hours after infarction. **F.** Biodistribution of ^{111}In-TO shows a 5-fold higher uptake in infarcted versus remote (septal) myocardium. TO conjugates are eliminated via both the renal and hepatic routes. **G-H.** The target to background ratio in the infarct (MI) is significantly increased with all TO probes. The TBR produced is highest with inversion recovery MRI of Gd-TO and lowest with Dex-TO. Conversely, CNR is significantly higher with Dex-TO. **p<0.01, ***p<0.001, ****p<0.0001, ns=not significant. FH=Feraheme.

Kinetics of NA release in IR

We next characterized the kinetics of NA release in myocardial ischemia-reperfusion (IR) by Dex-TO fluorescence. Near-infrared Annexin V (AV-750) was co-injected to detect cardiomyocyte apoptosis. Fluorescent microspheres were injected prior to reperfusion to define the area-at-risk (AAR). Mice were euthanized 2, 4, 6 or 24 hours after injury (n=6 per group). As shown in Figure 4A, the distribution of NA within the AAR was highly dynamic during the first 6 hours of reperfusion. At 2 hours the distribution of released NA correlated strongly with the distribution of apoptosis (AV-750) and filled much of the AAR. Thereafter, substantial washout of NA was seen, and by 4 hours the extent of myocardium positive for NA release was far smaller than the extent of apoptosis in the AAR (Figure 4B, C). The washout of released NAs from the AAR was largely complete within 4 hours, and the distribution of Dex-TO at this time resembled final infarct size (Figure 4D).

Anti-inflammatory and cytoprotective effects of Dex-TO

The initial broad distribution of NAs in the AAR, and their subsequent washout into the circulation,

motivated us to study the impact of Dex-TO on the immune response to injury. We first exposed Dex-TO to a panel of pro-inflammatory NAs (Figure 5A-D) to confirm its affinity and determine the EC_{50}. Mouse heart RNA had an EC_{50} of 6.5 µg/ml, while yeast RNA had an EC_{50} of 4.1 µg/ml. CpG DNA, a synthetic ligand for Toll-like receptor 9 (TLR-9) had an EC_{50} of 100 nM (0.2 µg/ml), while bacterial DNA had an EC_{50} of 0.06 nM (60 pM, 0.2 µg/ml). We then exposed bone-marrow derived mouse macrophages to RNA, DNA, and lipopolysaccharide (LPS). This stimulated the production of the proinflammatory cytokines TNF-alpha, CXCL2 and IL-6 by the activated macrophages, but no impact on the anti-inflammatory cytokine IL-10 (Figure 5E) was seen.

The addition of 10 µM Dex-TO (DTO) to the solution containing the NA-exposed macrophages reduced the production of TNF-alpha, CXCL2, and IL-6 by the macrophages significantly. A dose of 100 µM of Dex-TO produced a 64-fold reduction in cytokine production (Figure 5E). Dex-TO did not reduce IL-10 production or LPS-induced cytokine production. This suggests that the anti-inflammatory effect of Dex-TO was mediated via specific scavenging of NA and interference with NA mediated stimulation of TLRs. Control amino-dextran (without

TO) caused an unexpected, but mild, increase in cytokine production. This is consistent with prior reports of immune stimulation by dextran in mice [17-19]. Of note, the same amino-dextran preparation was used to synthesize Dex-TO, making the large reductions in cytokine production produced by Dex-TO even more noteworthy.
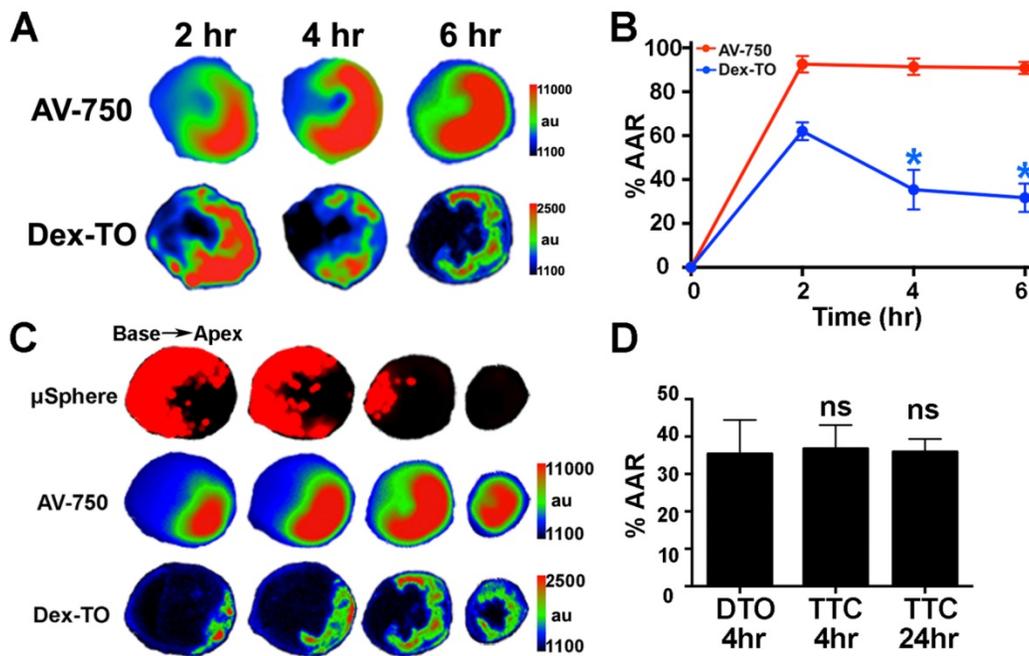

Figure 4: Dynamic accumulation of Dex-TO and extracellular nucleic acids in ischemia-reperfusion injury. A. Images of Annexin V (AV-750) and Dex-TO accumulation in the area-at-risk (AAR) 2, 4 and 6 hours after reperfusion. The distribution of AV-750 remains fairly constant, while that of Dex-TO is highly dynamic. **B.** Dex-TO accumulates widely in the AAR at 2 hours but undergoes a significant degree of washout between 2-4 hours. **C.** Images of a heart subjected to ischemia-reperfusion at 6 hours. The majority of the AAR is annexin positive (red-green) but a far smaller portion is Dex-TO positive. **D.** Infarct size after 35 minutes of ischemia-reperfusion determined by Dex-TO (DTO) injection, TTC staining at 4 hours and TTC at 24 hours. No significant difference is seen among the groups.
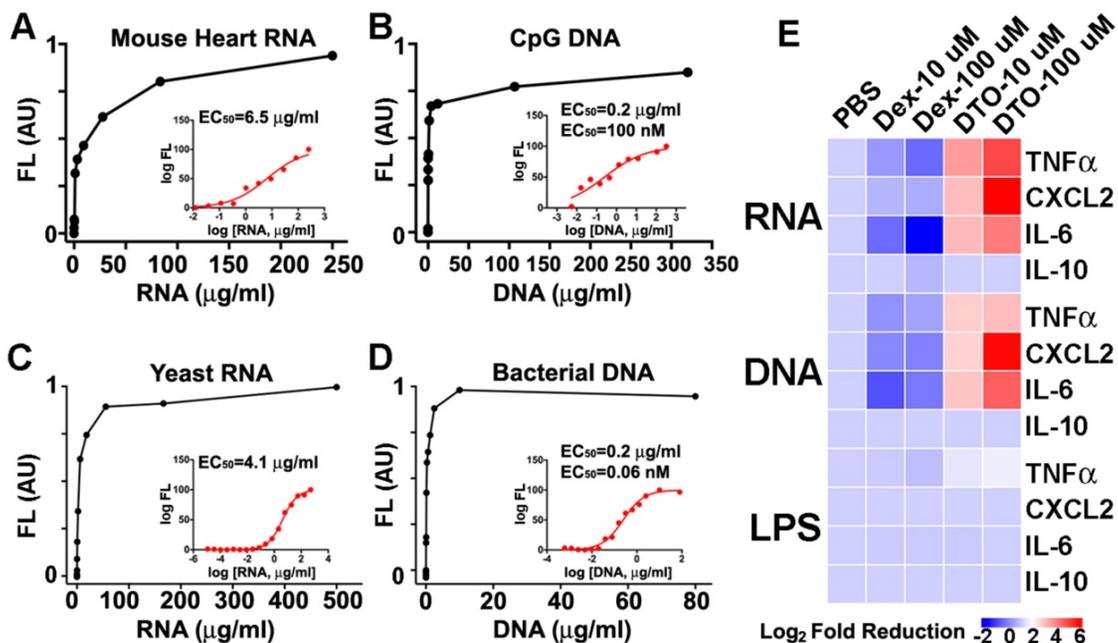

Figure 5: Dex-TO ameliorates the nucleic acid induced inflammatory response. A-D. Dex-TO fluorescence increases in the presence of proinflammatory nucleic acid species: mouse heart RNA (A), CpG DNA (B), yeast RNA (C), and bacterial DNA (D). The inset shows corresponding dose response curves and the EC_{50} values. **E.** Dex-TO (DTO) reduces the production of TNF-alpha, CXCL2 and IL-6 by activated macrophages exposed to mouse heart RNA or CpG DNA in a dose dependent fashion. Dex-TO has no effect on the production of IL-10, or on cytokine release induced by LPS. The color scale used plots the log_2 fold reduction in cytokine release, referenced to PBS. Control amino-dextran (without TO) causes a mild increase in cytokine production. In contrast, 100 μM of Dex-TO produces up to a 64-fold reduction in cytokine production.
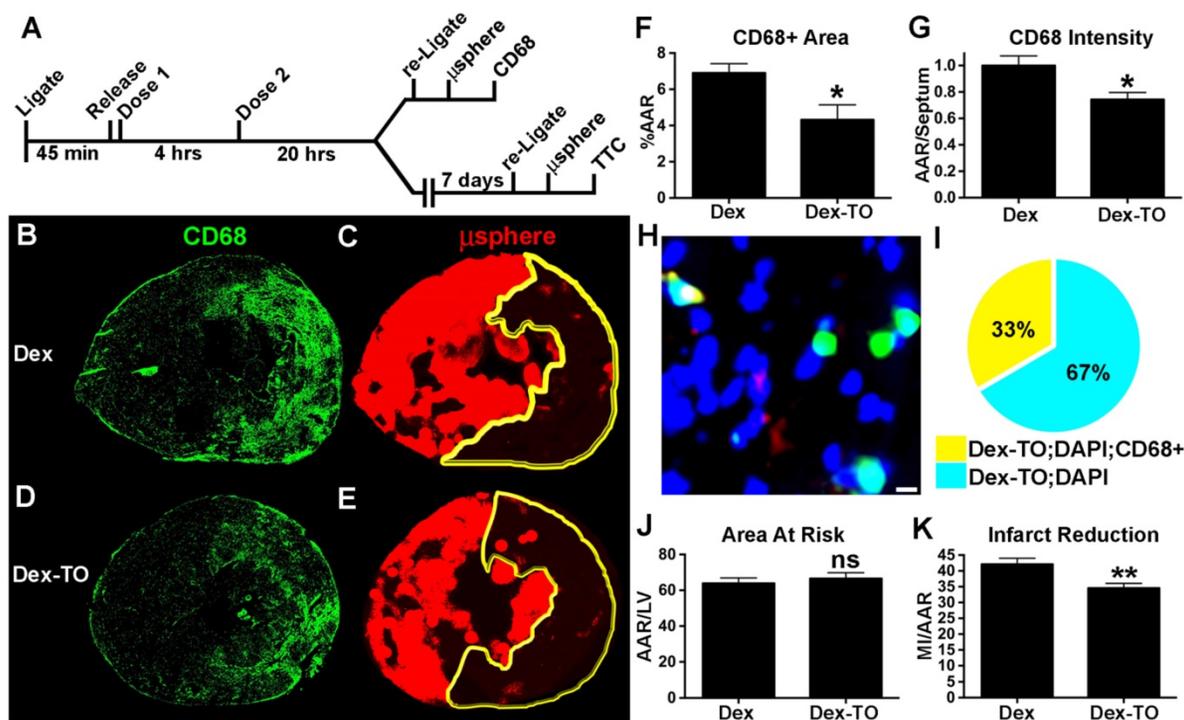
Figure 6: Dex-TO reduces inflammation and final infarct size in ischemia- reperfusion injured hearts. A. Protocol of the Dex-TO dosing regimen and the endpoints at 24 hrs (CD68 immunohistochemistry), and at 7 days (TTC staining). **B.** In control mice, a dense infiltrate of CD68 positive cells was seen at 24 hours throughout the area-at-risk (AAR), delineated in **C.** by the absence of microspheres (yellow outline). **D-E.** The infiltration of CD68 positive cells into the AAR at 24 hours was markedly reduced by Dex-TO injection. **F-G.** Dex-TO significantly reduced the CD68 positive portion of the AAR by 37% and CD68 fluorescence by 26%. **H-I.** Fluorescence microscopy of a Dex-TO treated heart co-stained with CD68 (red) and DAPI (blue). Dex-TO fluorescence (green) is seen in a subset of cells (turquoise), and of those only a fraction, 33% (I), are CD68 positive (yellow). White bar=5μm. **J.** No difference in the AAR was seen between the Dex-TO and Dex cohorts. **K.** A significant 18% reduction in infarct size was seen on day 7 with Dex-TO treatment. * $p<0.05$, ** $p<0.01$.

We subsequently developed a therapeutic regimen to scavenge cell-free NAs during the first 4 hours of IR with Dex-TO. After 45-min of ischemia, Dex-TO (10 nmol) was injected intravenously at the onset of reperfusion and again 4 hours later (Figure 6A). Control mice with IR were injected with an equivalent amount of Dextran (Dex). Half the mice were used to study the impact of Dex-TO injection on myocardial macrophage infiltration at 24 hours. The left coronary artery in these mice was religated at 24 hours and fluorescent microspheres were injected to delineate the AAR. The mice (7 control and 7 Dex-TO treated) were euthanized 5 minutes after the injection of the microspheres and the hearts were sectioned and stained with CD68, a surface marker for infiltrating leukocytes (predominantly macrophages at 24 hours) that remains elevated in both mice and humans with healing myocardial infarcts [20, 21]. The infiltration of CD68 positive cells was significantly reduced in the mice injected with Dex-TO (Figure 6B, G). High magnification microscopy of a Dex-TO treated heart is shown in Figure 6H and the results are summarized in Figure 6I. All Dex-TO positive foci colocalized with DAPI, while only 33% colocalized with CD68 positive cells. This suggests that the attraction of CD68 positive cells to released NAs was attenuated by Dex-TO.

The impact of Dex-TO on final infarct size was tested in 14 mice (7 control and 7 Dex-TO treated). The treatment regimen on day 1 was as above, and infarct size was assessed on day 7 (Figure 6A). The left coronary artery was religated on day 7 (five minutes prior to euthanasia), fluorescent microspheres were injected to delineate the AAR, and infarct size was assessed with TTC. No significant difference was seen in the AAR between the two groups (Figure 6J). However, Dex-TO treatment significantly reduced infarct size by 18% (Figure 6K). Taken together, these results show that Dex-TO given within 4 hours of reperfusion injury is anti-inflammatory and cardio-protective.

Discussion

Cell rupture and the exposure of NAs to the immune system can result from a variety of insults including ischemia, mechanical trauma, toxins, burns, sepsis, transplant rejection and autoimmune disease. Released NAs are highly pro-inflammatory and result in further tissue damage due to their excessive stimulation of the immune response. Here we describe Dex-TO, a multivalent NA-binding nanoprobe that can be used to detect tissue injury,

and further can exert anti-inflammatory and cytoprotective effects at the site of injury. The theranostic (diagnostic and therapeutic) capabilities of Dex-TO provide a new paradigm for the rapid diagnosis and simultaneous treatment of tissue injury.

Dex-TO constitutes a new class of anti-inflammatory drugs, a theranostic fluorescent nanoprobe. The fluorescent nature of the probe allows its disposition in cells and mechanism of action to be accurately determined. The intercalation of Dex-TO with NAs provides a stable and specific signature of NA binding as well as a mechanism of signal amplification. Free NAs form large nanoclusters upon binding to Dex-TO, which markedly reduces their ability to stimulate cytokine release from activated leukocytes. This attenuates further macrophage infiltration into the site of injury and ultimately reduces the extent of injury. An 18% reduction in day-seven myocardial infarct size was produced by Dex-TO, which compares extremely favorably with the reduction in infarct size produced by other anti-inflammatory approaches, such as siRNA to the chemokine receptor CCR2 [22].

The therapeutic effect of Dex-TO is based on its specific intercalation with NAs, which is an improvement over DNA scavenging polymers that rely on electrostatic forces [23, 24]. The positive charge of these polymers can potentially attenuate NA immunogenicity but can also result in non-specific binding to the many sources of negative charge in vivo, including peptidoglycans (e.g. heparin), negatively charged lipids, cell membranes and proteins (albumin). Nevertheless, recent studies have shown that DNA scavenging materials relying on electrostatic forces can be used to treat thrombosis [23], block DNA binding to anti-DNA antibodies in systemic lupus erythematosus [24], and modulate the innate immune response [25]. However, none of the electrostatic scavengers reported to date have the theranostic capability of Dex-TO, and the ability to combine a diagnostic imaging readout with efficient NA scavenging.

The attenuation of NA-induced tissue injury has also been attempted with DNase, RNase, small chemicals, and TLR inhibitors [7, 8, 26-31]. These agents, however, have short serum half-lives, need to be administered frequently and at a high dose, and are costly. RNase injected intravenously may also not be effectively delivered into the interstitial space where the extracellular NAs are released. Dex-TO, in addition to its theranostic nature, has several advantages over these approaches. Dex-TO scavenges both DNA and RNA and acts upstream of pathways in the innate immune response that are stimulated by NAs. The efficiency of Dex-TO binding to NA is extremely high, with an EC_{50} as low as 0.06 nM for bacterial DNA. In addition, Dex-TO is devoid of trace metals and high therapeutic doses could potentially be used without the risk of toxicity.

The current Dex-TO nanoprobe consists of a 40 kDa dextran carrier to which three TO molecules are attached. A 40 kDa carrier was selected based on studies of dextran pharmacokinetics in mice, which indicate that this dextran undergoes rapid extravasation along with moderately slow excretion [32, 33]. The ability to select different polymeric carriers and NA binding fluorochromes could allow a library of NA binding theranostics, each optimized for specific conditions, to be developed in the near future.

The utility of theranostic fluorescent nanoprobes, such as Dex-TO, will likely be greatest in organs that can be imaged with surface fluorescence imaging or endoscopy. This includes the retina, skin, lungs, urogenital and gastrointestinal tracts. Fluorescence imaging is being increasingly used in open surgical procedures and Dex-TO could play an important role in this context too. Dex-TO could prove particularly valuable for the early diagnosis and treatment of traumatic injury by early responders in the field. In addition, its extremely high affinity for bacterial DNA may make it particularly effective in the treatment of sepsis. The promise of Dex-TO thus extends from the basic investigation of disease pathophysiology to a new theranostic paradigm with a high potential for clinical translation.

Materials and Methods

Dex-TO synthesis and characterization

Synthesis: 1.4 µmol of TO-NHS ester (synthesized in-house as previously described [14]) was prepared in 100 µl anhydrous DMSO, and added immediately to 5.4 mg of amino-dextran 40kDa (Thermo Fisher Scientific, Waltham, MA) in 0.4 ml 1xDPBS. The reaction was incubated at 37ºC for 3 hours. After the solution had cooled down to room temperature, it was loaded on a PD-10 column, and eluted with 1mM phosphate buffer (pH 7.0). The final product was collected and reconstituted into 1mM phosphate buffer (2 ml). A light red powder was obtained after lyophilization. Dex-Cy5.5 was similarly synthesized by conjugating amino-dextran to Cy5.5-NHS ester (GE Healthcare, Little Chalfont, UK). A light blue powder was obtained after lyophilization.

TO valency determination: Dex-TO solution was prepared at 2.2 µM (0.26 µmol isomaltose unit in 1 ml of 1 x DPBS pH 7.4). 5 units of 400-800 units/mg lyophilized dextranase from *Penicillium sp.* (Sigma-Aldrich, St. Louis, MO), was prepared in 6 µl 1

x DPBS, and added to the Dex-TO solution. Reaction kinetics were measured by UV spectra from 250 nm to 750 nm, on an Evolution 300 UV-Vis spectrometer (Thermo Scientific), and recorded at 0, 1, 2, and 20 hours after incubation at 37°C. The TO concentration was calculated according to the absorbance at 509 nm and an extinction coefficient of 63,000 $M^{-1}cm^{-1}$ as previously described [34].

Dex-TO size measurement by FPLC: The dynamically based molecular size (hydrodynamic volume) of Dextran-TO was determined by Fast Protein Liquid Chromatography (FPLC) using an ÄKTA Purifier 10 and Superdex 200 10/300GL column (GE Healthcare) with a running buffer of 0.05 M sodium phosphate, 0.15 M NaCl (0.1% Tween, pH 7.2) and flow rate of 0.8 ml/min. Gel filtration calibration standards (GE Healthcare) including conalbumin (C), ovalbumin (O), carbonic anhydrase (CA), RNase A (R), aprotinin (Apr) were run to obtain a standard curve, with size exclusion retention determined by Blue Dextran 2000. The partition coefficient (K_{av}) was calculated as $K_{av} = (V_e-V_0) / (V_t-V_0)$, where Ve = elution volume, V_0 = void volume and Vt = total volume, and then plotted against the relative molecular weights (M_r) of the aforementioned standards. M_r of Dex-TO was determined from the standard curve.

In Vitro binding assays: Bacterial Phage Lambda DNA (Sigma-Aldrich), CpG DNA (Enzo Life, Plymouth Meeting, PA), Torula yeast RNA (Sigma-Aldrich) were completely dissolved in Tris-acetate-EDTA (TAE) buffer (pH = 8) by gentle inversion overnight at 4°C. Lambda DNA, CpG DNA, yeast RNA stock solutions were characterized by spectrophotometry to determine the concentration and purity. Total mouse heart RNA was extracted from C57Bl6 mouse hearts using TRI Reagent (Sigma-Aldrich) and characterized with a NanoDrop spectrophotometer (Thermo Fisher) as previously described [9].

To measure the fluorescence response in the presence of nucleic acid (NA), serial dilutions of the NA solutions with ratio of 1:3 were prepared in a Corning Costar 96-Well black clear-bottom plate (Thermo Fisher). 50 nM of fluorochrome equivalents, based on the common benzothiazole ring, were added to the NA-containing wells and incubated for 2 hours. Fluorescence was measured with the GloMax-Multi Detection System and snap-in fluorescent optical kits (Promega, Madison, WI). EC_{50} was determined using the dose-response curve fitting function implemented in Prism (GraphPad, La Jolla, CA).

Flow Cytometry: Cardiomyocyte line HL-1 cells were seeded on a 24-well plate at 1×10^5 cells/well. Cell necrosis/membrane rupture was induced with 50

μM final concentration of 2,3-Dimethoxy-1,4-naphthoquinone (DMNQ, from Sigma-Aldrich). Healthy control cells were treated with PBS. After 24 hours of incubation, the cells were trypsinized and co-stained with Dex-TO (300 nM) and Sytox Blue (1 μM) at 37°C for 15min. After washing with 1 ml of DPBS, cells were pelleted, resuspended in 300 μl of DPBS, and analyzed with a 4 laser LSRII system (BD Biosciences, Franklin Lakes, NJ). Dex-TO was excited with the 488 nm solid state laser and emission detected with the 525/50 nm filter. Sytox was excited with the 405 nm violet laser and emission detected with the 450/50 nm filter. A compensation matrix was applied to correct for spectral overlap and signal spillover. Cytometry data was analyzed and scatterplots generated in Flowjo (Tree Star Inc., Ashland, OR).

Confocal Microscopy: HL-1 cells were treated with 50 μM DMNQ and co-stained with Dex-TO (300 nM final concentration) and Sytox blue (1 μM) for 15 min at room temperature. Confocal fluorescent images were acquired on a custom built 4-laser Zeiss Axio Observer Z1 inverted microscope (Carl Zeiss AG, Oberkochen, Germany) equipped with a confocal spinning-disk unit (CSU-X1) (Yokogawa, Musashino, Tokyo, Japan). Stained cells were observed using a 10X objective lens. Dex-TO was imaged with 425/20-25 nm excitation, 525/30 nm emission filter setting. Sytox blue was imaged with 387/11-25 nm excitation, 440/40 nm emission filter setting. Images were recorded using an Evolve 512 electron-multiplying charge-coupled device (EMCCD) camera (Photometrics, Tucson, AZ), with Slidebook 5.1 Software (Intelligent Imaging Innovations (3i), Denver, CO), and processed in ImageJ (NIH).

Dex-TO/DNA aggregate size measurement: A Lambda DNA dilution series was prepared as above and incubated with 50 nM fluorochrome equivalents of Dex-TO for 2 hours at 37°C. Hydrodynamic size of the Dex-TO/DNA microaggregates was then measured by dynamic light scattering using a Zetasizer (Malvern Instruments, Marlboro, MA).

^{111}In-TO-DTPA synthesis and characterization: In a 5 ml react vial, 1.663 mCi of $^{111}InCl_3$ stock solution (Nordion, Ottawa, Canada), diluted in 60 μl of 0.05 N HCl, was added to 0.8 mg (0.83 μmol) of TO-DTPA in 300 μl of 0.1 M acetic acid in a high purity water solution. The mixture was stirred at room temperature for 40 minutes. The labeling was validated by HPLC analysis of 10 μl of the reaction mixture, diluted into 500 μl of 0.1 M acetic acid in high purity water. HPLC was run on a Varian ProStar detector and delivery modules (Varian Medical Systems, Palo Alto, CA) with eluent A (0.1% TFA in

water), and a gradient of 10-50% eluent B (0.1%TFA with 90% acetonitrile in 9.9% water) in 10 min, back to 10% B in 5 min and isocratic for 5 min, flow: 5 ml/min, 500 nm on a C18 column. Radiochemical yield (RCY) was >99%; Specific Activity was 2 mCi/μmol. Immediately before injection, the ^{111}In-TO-DTPA solution was taken into a syringe, filtered through a 0.22 μm nylon filter, and washed with 267μl of sterilized 1xPBS.

Animal models and protocols

All experiments and procedures were performed in accordance with the National Institutes of Health's "Guide for the Care and Use of Laboratory Animals" and were approved by the Massachusetts General Hospital Institutional Animal Care and Use Committee.

Myocardial Infarction: Myocardial Infarction was induced in adult female C57Bl6 mice (Jackson Laboratory, Bar Harbor, ME) by permanent ligation of the left coronary artery (LCA) as previously described [15]. After 24 hours, a cohort of these mice (n=7) was co-injected intravenously with 10 nmol each of Dex-TO and Dex-Cy5.5 for fluorescence imaging. A second cohort was injected intravenously with 50 μCi of ^{111}In-TO (n=6) to assess myocardial uptake and biodistribution, as described below. A separate group of mice was injected intraperitoneally with 0.1 mmol/kg Gd-TO (n=6) within 24 hours of the ligation for MR imaging. T1 maps of Gd-TO uptake in these mice have previously been reported [15] but not TBR or CNR. CNR was calculated as $(signal_{infarct} - signal_{septum})/sd_{noise}$, where sd_{noise} was the standard deviation of the noise. TBR was defined as $signal_{infarct}/signal_{septum}$.

Myocardial ischemia-reperfusion: Ischemia-reperfusion (IR) injury was induced by transient occlusion of the LCA, followed by release of the suture to establish full reperfusion. The ECG was monitored to ensure that the ST segments remained elevated throughout the duration of occlusion. Mice core temperature was maintained at 38°C, and heart rate was maintained at 500 beats per minute. Reperfusion was confirmed visually and by resolution of the ST elevation. The released suture was left in place for subsequent religation and fluorescent microsphere injection, performed just prior to euthanasia, in order to delineate the area-at-risk (AAR).

To determine the kinetics of NA release in IR, mice were exposed to 35 minutes of transient occlusion of the LCA followed by reperfusion. Two hours prior to sacrifice, 10 nmol Dex-TO and 100 μl AV-750 (PerkinElmer, Waltham, MA) were co-injected into the tail vein. The mice were sacrificed

at 2, 4, 6 or 24 hours after injury (n=6 per group). Hearts were sectioned into 1-mm short axial slices and imaged with fluorescence reflectance imaging (FRI). To determine whether the scavenging of NAs by Dex-TO exerted a protective effect in IR, a more aggressive model involving 45 minutes of LCA ligation was used. In one cohort of these mice (n=14) Dex-TO (10 nmol I.V.) was injected at the time of reperfusion, and again 4 hours later. A control cohort (n=14) underwent the identical protocol but was injected with 10 nmol of unconjugatd 40 kDa dextran. After 24 hours, half of the mice in each cohort (n=7) were re-anesthetized, the LCA was re-ligated, and the mice were injected with fluorescent microspheres 5 minutes prior to euthanasia. The excised hearts were embedded and cryo-sectioned for immunohistochemistry. The remaining mice (n=7 per cohort) were allowed to recover for 7 days at which time the LCA was re-ligated, followed immediately by microsphere injection and euthanasia. The excised hearts in these mice were sectioned axially into 1-mm slices for AAR assessment and TTC staining.

Mice cohorts imaged: A total of 11 cohorts of mice were imaged:

- Permanent occlusion of LCA - injection of Dex-TO, Dex-Cy5.5, and microspheres at 24 hours (n=7).
- Permanent occlusion of LCA - injection of Gd-TO within 24 hours (n=6).
- Permanent occlusion of LCA - injection of ^{111}In-TO at 24 hours (n=6).
- 35-minute IR co-injected with Dex-TO, AV-750 and microspheres, in mice 2 hrs (n=6), 4hrs (n=6), 6hrs (n=6), and 24hrs (n=6) after reperfusion.
- 45-minute IR injected with Dex-TO at reperfusion and at 4 hours – hearts sectioned for CD68 staining at 24 hours (n=7).
- 45-minute IR injected with control Dex at reperfusion and at 4 hours – hearts sectioned for CD68 staining at 24 hours (n=7).
- 45-minute IR injected with Dex-TO at reperfusion and at 4 hours – hearts sectioned for TTC staining of final infarct size at 7 days (n=7).
- 45-minute IR injected with control Dex at reperfusion and at 4 hours – hearts sectioned for TTC staining of final infarct size at 7 days (n=7).

Imaging and biodistribution

Fluorescence lifetime imaging: Dex-TO (300 nM final concentration) with or without Lambda DNA, and a control sample containing buffer only were incubated at 37°C, for 2 hours before imaging. In addition, mice after 24 hours of permanent LCA ligation were co-injected intravenously with Dex-TO and Dex-Cy5.5 (10 nmol each), which were allowed to

circulate for 2 hours prior to euthanasia. The hearts were then harvested and sectioned into 1-mm axial slices for fluorescence lifetime imaging and TTC staining. Time resolved imaging of heart slices was performed with a custom-built imaging system described in detail previously [35]. Briefly, fluorescence was excited with the direct output of a pulsed broadband (480 to 850 nm) Mai Tai titanium sapphire laser with 80 MHz repetition rate (Spectra-physics, Santa Clara, CA), photonic crystal fiber (Thorlabs, Newton, NJ) filtered through either the 495±25nm (Dex-TO) or 650/40 nm (Dex-Cy5.5) filter. The resulting fluorescence emission was detected with either a 529±25nm filter (Dex-TO), or a 700-nm long pass filter (Dex-Cy5.5), both coupled to an intensified 12-bit cooled CCD camera with a 300–500 ps gate width, 600 V gain, 150 ps steps and 4 × 4 hardware binning (LaVision GmbH, Goettingen, Germany). The gated intensified CCD camera provided 200 ps time resolution with a 2 x 2 cm^2 field-of-view. Excitation powers were 50 µW/cm^2 at both 495 and 650 nm, and camera integration times ranged from 100 ms to 3 s.

Continuous wave fluorescence imaging: Heart slices sectioned along the short axis were imaged on a commercial imaging system (IVIS Spectrum, PerkinElmer). Dex-TO fluorescence was detected with an excitation wavelength of 500 nm, emission wavelength of 540 nm and a 30-sec exposure time. Dex-Cy5.5 fluorescence was detected with an excitation wavelength of 675 nm, emission wavelength of 720 nm and a 30-sec exposure time. Microsphere fluorescence was detected with an excitation wavelength of 570 nm, emission wavelength of 620 nm and a 20-sec exposure time. AV-750 fluorescence was detected with an excitation wavelength of 745 nm, emission wavelength of 800 nm and a 30-sec exposure time. All images were acquired at a spatial resolution of 135 µm. Fluorescence intensity was quantified and analyzed in ImageJ (NIH, Bethesda MD).

Molecular magnetic resonance imaging (MRI): Mice within 24 hours of permanent LCA ligation were injected with Gd-TO (0.1 mmol/kg ip). After 3 hours of probe circulation, Gd-TO enhanced MRI was performed on a 9.4 Tesla horizontal bore magnet (Biospec, Bruker, Billerica MA). T1 maps were acquired as previously described [15]. In addition, gradient echo cines were acquired in the short axis of the left ventricle using cardiorespiratory gating (SA Instruments, Stonybrook, NY) and the following settings: Slice 1mm, FOV 25x25mm, Matrix 200 x 200, flip angle 30 degrees, 20 frames per RR interval, TE 1ms, 4 averages. CNR and TBR were derived from these gradient echo cines, as described above.

Biodistribution: 50 µCi of ^{111}In-TO was injected intravenously into each mouse. The actual injected dose (ID) was determined by subtracting the residual radioactivity after injection from the dose prepared before injection. Tissues were harvested after 3 hours of tracer circulation time. Radioactivity in tissue was quantified as counts per minute (CPM), measured by a Wallac 1480 wizard gamma counter and Packard Tri-Carb liquid scintillation analyzer (Perkin Elmer). The tissue uptake was expressed as percentage of injected dose per gram of tissue (%ID/g).

Infarct Size and histology

Infarct size measurement: Excised hearts were sectioned axially into 1 mm thickness (McIlwain 800 Series, Vibratome, St Louis, MO) and stained with 2,3,5-triphenyltetrazolium chloride (TTC, from GFS Chemicals, Powell, OH) following the manufacturer's protocol. TTC images were acquired on a flatbed scanner (Hewlett Packard, Palo Alto, CA), and microsphere images were acquired on the IVIS spectrum. Image analysis was performed in ImageJ, with infarction size across the heart slices normalized to the area-at-risk (AAR).

Immunohistochemistry: Excised hearts were embedded in Optimal Cutting Temperature compound (OCT, from Thermo Fisher), and 10 µm short-axis cryo-sections were collected. Direct immunohistochemistry of CD68 was performed with anti-CD68 antibody conjugated to Alexa Fluor 647 fluorophore (Santa Cruz Biotechnology, Dallas, TX) per manufacturer's instructions. Diamidino-2-phenylindole (DAPI, from Thermo Fisher) staining was performed to visualize the nuclei. Microscopy was performed on a TISSUEFAXS system (TissueGnostics GmbH, Vienna, Austria), with a 40X objective lens (Zeiss), DAPI (for DAPI), GFP (for Gd-TO), and Alexa 647 (for CD68) filter settings. Images were acquired on a 12 bit CCD camera (Pixelink, Ottawa, Ontario, Canada), with the TissueFAXS image acquisition software, and analyzed in Image J (NIH).

Macrophage Cytokine Production

Multiplexed cytokine assay: Bone marrow cells were harvested from the tibias and femurs of C57Bl6 mice and seeded in a 96-well plate at 2 x 10^5 cells/well, as previously described [9]. Cells were cultured in supplemented RPMI 1640 medium in the presence of 10 ng/ml macrophage colony-stimulating factor (R&D systems, Minneapolis, MN) to induce differentiation into bone marrow derived macrophages (BMDMs). On day 5, the BMDMs were exposed to a variety of stimuli including CpG DNA, purified mouse heart RNA, and Lipopolysaccharides

(LPS) from *Escherichia coli* (Sigma-Aldrich). The BMDMs were exposed to the stimuli in culture. After 24 hrs, cytokine production in the culture medium was measured.

The culture media from the stimulated BMDMs were collected and stored at -80°C for cytokine protein measurements. CXCL2 levels were measured with a commercial ELISA kit (R&D systems, Minneapolis, MN) following manufacturer's instructions. TNF-alpha, IL-6 and IL-10 concentrations were determined using a fluorescent bead-based multiplex immunoassay (Luminex, Austin, TX). Briefly, an antibody for each cytokine was covalently immobilized to a set of fluorescent microspheres by the manufacturer (Millipore, Billerica, MA). After overnight incubation, cytokines bound on the surface of the microspheres were detected by the mixture of biotinylated antibodies. After binding of streptavidin-phycoerythrin conjugates, the reporter fluorescent signal was measured with a Luminex 200 reader (Luminex). Final cytokine concentrations were calculated based on a standard curve constructed for each experiment. Cytokine production by DNA, RNA and LPS was measured under several conditions. To determine whether Dex-TO would decrease cytokine production, the nanoprobe was added to the culture medium to produce concentrations of 10μM or 100μM of Dex-TO. Control conditions included adding 10μM of Dextran, 100μM of Dextran or PBS to the medium.

Abbreviations

TO: thiazole orange; Dex-TO/DTO: dextran-thiazole orange conjugate; NA: nucleic acid; TLR: Toll-like receptor; FH: feraheme; NHS: N-hydroxysuccinimide; FPLC: Fast Protein Liquid Chromatography; FRI: fluorescence reflectance imaging; ROC: receiver operating characteristic; TTC: 2,3,5-triphenyltetrazolium chloride; AUC: area under the curve; DTPA: diethylene triamine pentaacetic acid; CNR: contrast to noise ratio; IR: ischemia-reperfusion; AV-750: Annexin V-near-infrared fluorochrome; AAR: area-at-risk; LPS: lipopolysaccharide; Dex: dextran; CCR2: C-C chemokine receptor type 2.

Acknowledgments

Competing Interests

The authors have declared that no competing interest exists.

References

1. Rahman A, Isenberg DA. Systemic lupus erythematosus. N Engl J Med. 2008; 358: 929-39.
2. Rainer TH, Wong LK, Lam W, Yuen E, Lam NY, Metreweli C, et al. Prognostic use of circulating plasma nucleic acid concentrations in patients with acute stroke. Clin Chem. 2003; 49: 562-9.
3. Lam NY, Rainer TH, Chan LY, Joynt GM, Lo YM. Time course of early and late changes in plasma DNA in trauma patients. Clin Chem. 2003; 49: 1286-91.
4. Logters T, Paunel-Gorgulu A, Zilkens C, Altrichter J, Scholz M, Thelen S, et al. Diagnostic accuracy of neutrophil-derived circulating free DNA (cf-DNA/NETs) for septic arthritis. J Orthop Res. 2009; 27: 1401-7.
5. Margraf S, Logters T, Reipen J, Altrichter J, Scholz M, Windolf J. Neutrophil-derived circulating free DNA (cf-DNA/NETs): a potential prognostic marker for posttraumatic development of inflammatory second hit and sepsis. Shock. 2008; 30: 352-8.
6. Chang CP, Chia RH, Wu TL, Tsao KC, Sun CF, Wu JT. Elevated cell-free serum DNA detected in patients with myocardial infarction. Clin Chim Acta. 2003; 327: 95-101.
7. Cavassani KA, Ishii M, Wen H, Schaller MA, Lincoln PM, Lukacs NW, et al. TLR3 is an endogenous sensor of tissue necrosis during acute inflammatory events. J Exp Med. 2008; 205: 2609-21.
8. Chen C, Feng Y, Zou L, Wang L, Chen HH, Cai JY, et al. Role of extracellular RNA and TLR3-Trif signaling in myocardial ischemia-reperfusion injury. J Am Heart Assoc. 2014; 3: e000683.
9. Feng Y, Chen H, Cai J, Zou L, Yan D, Xu G, et al. Cardiac RNA induces inflammatory responses in cardiomyocytes and immune cells via Toll-like receptor 7 signaling. J Biol Chem. 2015; 290: 26688-98.
10. Brentano F, Schorr O, Gay RE, Gay S, Kyburz D. RNA released from necrotic synovial fluid cells activates rheumatoid arthritis synovial fibroblasts via Toll-like receptor 3. Arthritis Rheum. 2005; 52: 2656-65.
11. Lim DM, Wang ML. Toll-like receptor 3 signaling enables human esophageal epithelial cells to sense endogenous danger signals released by necrotic cells. Am J Physiol Gastrointest Liver Physiol. 2011; 301: G91-9.
12. Zou L, Feng Y, Xu G, Jian W, Chao W. Splenic RNA and MicroRNA Mimics Promote Complement Factor B Production and Alternative Pathway Activation via Innate Immune Signaling. J Immunol. 2016; 196: 2788-98.
13. Cho H, Alcantara D, Yuan H, Sheth RA, Chen HH, Huang P, et al. Fluorochrome-functionalized nanoparticles for imaging DNA in biological systems. ACS Nano. 2013; 7: 2032-41.
14. Garanger E, Hilderbrand SA, Blois JT, Sosnovik DE, Weissleder R, Josephson L. A DNA-binding Gd chelate for the detection of cell death by MRI. Chem Commun (Camb). 2009: 4444-6.
15. Huang S, Chen HH, Yuan H, Dai G, Schuhle DT, Mekkaoui C, et al. Molecular MRI of acute necrosis with a novel DNA-binding gadolinium chelate: kinetics of cell death and clearance in infarcted myocardium. Circ Cardiovasc Imaging. 2011; 4: 729-37.
16. Montet-Abou K, Daire JL, Hyacinthe JN, Jorge-Costa M, Grosdemange K, Mach F, et al. In vivo labelling of resting monocytes in the reticuloendothelial system with fluorescent iron oxide nanoparticles prior to injury reveals that they are mobilized to infarcted myocardium. Eur Heart J. 2010; 31: 1410-20.
17. Coutinho A, Moller G, Richter W. Molecular basis of B-cell activation. I. Mitogenicity of native and substituted dextrans. Scand J Immunol. 1974; 3: 321-8.
18. Duplancic B, Stambolija V, Holjevac J, Zemba M, Balenovic I, Drmic D, et al. Pentadecapeptide BPC 157 and anaphylactoid reaction in rats and mice after intravenous dextran and white egg administration. Eur J Pharmacol. 2014; 727: 75-9.
19. Blanckmeister CA, Sussdorf DH. Macrophage activation by cross-linked dextran. J Leukoc Biol. 1985; 37: 209-19.
20. Heidt T, Courties G, Dutta P, Sager HB, Sebas M, Iwamoto Y, et al. Differential contribution of monocytes to heart macrophages in steady-state and after myocardial infarction. Circ Res. 2014; 115: 284-95.
21. Lee WW, Marinelli B, van der Laan AM, Sena BF, Gorbatov R, Leuschner F, et al. PET/MRI of inflammation in myocardial infarction. J Am Coll Cardiol. 2012; 59: 153-63.
22. Leuschner F, Dutta P, Gorbatov R, Novobrantseva TI, Donahoe JS, Courties G, et al. Therapeutic siRNA silencing in inflammatory monocytes in mice. Nat Biotechnol. 2011; 29: 1005-10.
23. Jain S, Pitoc GA, Holl EK, Zhang Y, Borst L, Leong KW, et al. Nucleic acid scavengers inhibit thrombosis without increasing bleeding. Proc Natl Acad Sci USA. 2012; 109: 12938-43.
24. Stearns NA, Lee J, Leong KW, Sullenger BA, Pisetsky DS. The inhibition of anti-DNA binding to DNA by nucleic acid binding polymers. PLoS one. 2012; 7: e40862.
25. Holl EK, Shumansky KL, Pitoc G, Ramsburg E, Sullenger BA. Nucleic acid scavenging polymers inhibit extracellular DNA-mediated innate immune activation without inhibiting anti-viral responses. PLoS one. 2013; 8: e69413.

26. Vogel B, Shinagawa H, Hofmann U, Ertl G, Frantz S. Acute DNase1 treatment improves left ventricular remodeling after myocardial infarction by disruption of free chromatin. Basic Res Cardiol. 2015; 110: 15.

27. Fuchs TA, Brill A, Duerschmied D, Schatzberg D, Monestier M, Myers DD, Jr., et al. Extracellular DNA traps promote thrombosis. Proc Natl Acad Sci USA. 2010; 107: 15880-5.

28. Barrat FJ, Meeker T, Chan JH, Guiducci C, Coffman RL. Treatment of lupus-prone mice with a dual inhibitor of TLR7 and TLR9 leads to reduction of autoantibody production and amelioration of disease symptoms. Eur J Immunol. 2007; 37: 3582-6.

29. Plitas G, Burt BM, Nguyen HM, Bamboat ZM, DeMatteo RP. Toll-like receptor 9 inhibition reduces mortality in polymicrobial sepsis. J Exp Med. 2008; 205: 1277-83.

30. Cabrera-Fuentes HA, Ruiz-Meana M, Simsekyilmaz S, Kostin S, Inserte J, Saffarzadeh M, et al. RNase1 prevents the damaging interplay between extracellular RNA and tumour necrosis factor-alpha in cardiac ischaemia/reperfusion injury. Thromb Haemost. 2014; 112: 1110-9.

31. Shak S, Capon DJ, Hellmiss R, Marsters SA, Baker CL. Recombinant human DNase I reduces the viscosity of cystic fibrosis sputum. Proc Natl Acad Sci USA. 1990; 87: 9188-92.

32. Dreher MR, Liu W, Michelich CR, Dewhirst MW, Yuan F, Chilkoti A. Tumor vascular permeability, accumulation, and penetration of macromolecular drug carriers. J Natl Cancer Inst. 2006; 98: 335-44.

33. Takakura Y, Hashida M. Macromolecular carrier systems for targeted drug delivery: pharmacokinetic considerations on biodistribution. Pharm Res. 1996; 13: 820-31.

34. Nygren J, Svanvik N, Kubista M. The interactions between the fluorescent dye thiazole orange and DNA. Biopolymers. 1998; 46: 39-51.

35. Kumar AT, Raymond SB, Dunn AK, Bacskai BJ, Boas DA. A time domain fluorescence tomography system for small animal imaging. IEEE Trans Med Imaging. 2008; 27: 1152-63.